



Contents lists available at ScienceDirect

## Optics and Laser Technology

journal homepage: [www.elsevier.com/locate/optlastec](http://www.elsevier.com/locate/optlastec)

Full length article

## Impact of initial pulse shape on the nonlinear spectral compression in optical fibre

Sonia Boscolo<sup>a</sup>, Frederic Chaussard<sup>b</sup>, Esben Andresen<sup>c</sup>, Hervé Rigneault<sup>d</sup>, Christophe Finot<sup>b,\*</sup><sup>a</sup> Aston Institute of Photonic Technologies, School of Engineering and Applied Science, Aston University, Birmingham B4 7ET, United Kingdom<sup>b</sup> Laboratoire Interdisciplinaire Carnot de Bourgogne, UMR 6303 CNRS-Université de Bourgogne-Franche-Comté, 9 avenue Alain Savary, BP 47870, 21078 Dijon Cedex, France<sup>c</sup> Univ. Lille, CNRS, UMR 8523 – PhLAM – Physique des Lasers Atomes et Molécules, F-59000 Lille, France<sup>d</sup> Institut Fresnel, CNRS, Aix-Marseille Université, Ecole Centrale Marseille, Campus de Saint Jérôme, F-13397 Marseille Cedex 20, France

## ARTICLE INFO

## Article history:

Received 13 April 2017

Accepted 14 August 2017

Available online xxxx

## Keywords:

Nonlinear spectral compression

Nonlinear fiber optics

Pulse shaping

## ABSTRACT

We theoretically study the effects of the temporal intensity profile of the initial pulse on the nonlinear propagation spectral compression process arising from nonlinear propagation in an optical fibre. Various linearly chirped input pulse profiles are considered, and their dynamics is explained with the aid of time-frequency representations. While initially parabolic-shaped pulses show enhanced spectral compression compared to Gaussian pulses, no significant spectral narrowing occurs when initially super-Gaussian pulses are used. Triangular pulses lead to a spectral interference phenomenon similar to the Fresnel bi-prism experiment.

© 2017 Elsevier Ltd. All rights reserved.

## 1. Introduction

Self-phase modulation (SPM) in optical fibre is ordinarily associated with spectral broadening of an ultra-short optical pulse. However, for appropriate initial conditions of the input pulse, SPM can result in significant spectral compression [1]. Indeed, SPM causes spectral compression or broadening depending on the initial frequency modulation (chirp) of the pulse electric field. Specifically, a pulse with a negative chirp, such as that imparted by an anomalously dispersive element, is compressed by the effects of SPM [2–4]. This method of spectral compression has been implemented using various types of fibres [5–8] and has also been studied in nonlinear waveguides [9]. It is suitable for a very large range of wavelengths including Ti:sapphire wavelengths [5,8], the widely used 1- $\mu\text{m}$  [7,10,11] and 1.55- $\mu\text{m}$  [12] windows and the emerging 2- $\mu\text{m}$  band [13]. The process can also sustain simultaneous amplification of the pulse [10,11,13,14], thereby providing an attractive solution to convert ultra-short pulses delivered by femtosecond oscillators into high-power, near-transform-limited picosecond pulses, and to counteract the spectrum expansion that usually occurs with the direct amplification of picosecond structures.

Most of the theoretical and experimental works to date have considered usual initial pulse profiles such as Gaussian or hyperbolic secant pulses [3,5,8,10,11,14]. However, several recent stud-

ies have demonstrated that the use of pre-shaped input pulses with a parabolic waveform can achieve spectral compression to the Fourier transform limit owing to the fact that for such pulses the cancellation of the linear and nonlinear phases can be made complete [15–17]. The purpose of this paper is to provide insight into the influence of the input temporal intensity profile on the spectral dynamics of negatively chirped pulses that occurs upon nonlinear propagation in a fibre. In particular, we emphasize that spectral narrowing does not occur for any initial pulse shape, and that there are significant differences between the propagation of parabolic, Gaussian, super-Gaussian or triangular pulses, which we elucidate with the aid of a time-frequency analysis. We show that initially parabolic-shaped pulses provide the best results in terms of quality of the compressed spectrum. Initially Gaussian pulses undergo efficient spectral compression, but the resulting spectrum exhibits residual pedestals stemming from uncompensated higher-order phase. On the contrary, super-Gaussian pulses do not experience any spectral narrowing, and their spectral extent does not change significantly upon propagation. In the case of triangular pulses, we observe a spectral interference phenomenon similar to Fresnel bi-prism interference. Simple analytic formulae are presented, which can predict the evolution of the spectral extent of the different input pulses along the fibre. We also discuss the impact of realistic initial conditions and system parameters on the spectral dynamics, and show that the interference pattern observed with triangular pulses is strongly affected by deviations of the initial waveform from the ideal shape.

\* Corresponding author.

E-mail address: [christophe.finot@u-bourgogne.fr](mailto:christophe.finot@u-bourgogne.fr) (C. Finot).

## 2. Ideal nonlinear propagation of differently shaped pulses

### 2.1. Situation under investigation

In this section, we study the propagation in a nonlinear optical fibre of initially perfect pulse waveforms with a negative linear chirp, given by  $\psi_{in}(t) = \sqrt{P I_{in}(t)} \exp(-iAt^2/2)$ . Here,  $I_{in}(t)$  is the temporal intensity profile of the pulse,  $P$  is the pulse peak power, and  $A$  is the chirp coefficient. We assume that these pulses have been temporally stretched in an anomalously dispersive medium so as to acquire a parabolic temporal phase over far-field evolution. For the purpose of illustration, we consider pulses at the wavelength 1550 nm, with a full-width at half maximum (FWHM) duration  $T_{fwhm} = 100$  ps (after dispersive temporal broadening) and  $A = -16.7 \times 10^{-3}$  rad.ps $^{-2}$ , yielding a spectral FWHM bandwidth  $\Omega_{fwhm,0} \approx |A|T_{fwhm}$  in the far-field regime. Four ideal and symmetric pulse shapes are investigated: a parabolic pulse with  $I_P(t) = (1 - t^2/T_P^2)\theta(T_P - |t|)$ , a Gaussian pulse with  $I_G(t) = \exp(-t^2/T_G^2)$ , a fourth-order super-Gaussian pulse approaching rectangular shape with  $I_S(t) = \exp(-t^8/T_S^8)$ , and a triangular waveform where  $I_T(t) = (1 - |t|/T_T)\theta(T_T - |t|)$ . Here,  $\theta(x)$  is the Heaviside function. The characteristic temporal values  $T_P$ ,  $T_G$ ,  $T_S$  and  $T_T$  can be related to the FWHM pulse duration as  $T_P = T_{fwhm}/\sqrt{2}$ ,  $T_G = T_{fwhm}/2\sqrt{\ln 2}$ ,  $T_S = T_{fwhm}/2(\ln 2)^{1/8}$ , and  $T_T = T_{fwhm}$ . The peak power is set to 12.5 W for the parabolic, Gaussian and super-Gaussian pulses and to 40 W for the triangular pulse. Fig. 1 shows the temporal and spectral intensity profiles of the initial pulses.

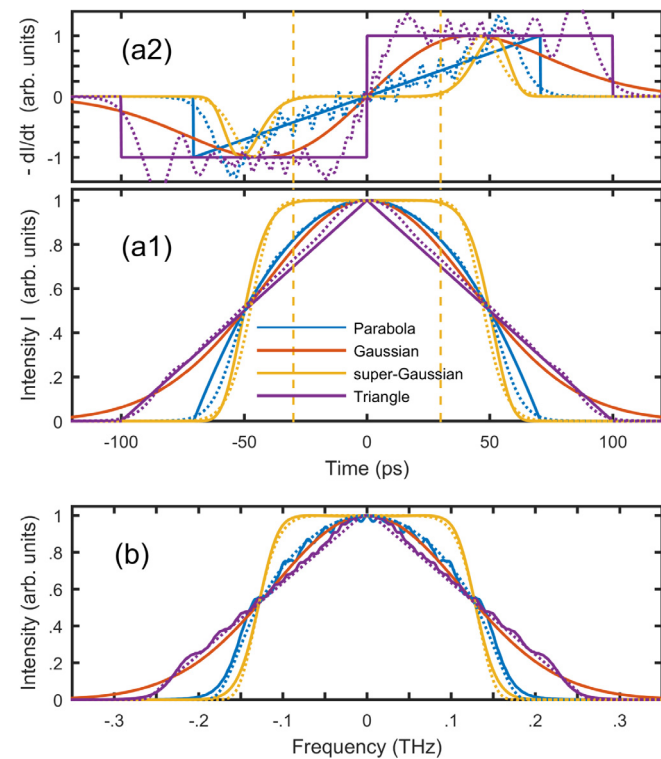


**Fig. 1.** (a) Temporal intensity profiles (subplot 1) and temporal intensity gradients (subplot 2), and (b) spectral intensity profiles of parabolic (blue), Gaussian (red), fourth-order super-Gaussian (orange) and triangular (violet) pulses at the entrance of the fibre. The ideal waveforms are plotted with solid lines while the results obtained through frequency-to-time shaping (see Section 4) are plotted with dotted lines. The vertical orange dashed lines in panels a delimit the region where the intensity distribution of the super-Gaussian pulse can be reasonably considered as flat. (For interpretation of the references to colour in this figure legend, the reader is referred to the web version of this article.)

Our numerical simulations of pulse propagation in the fibre are based on the standard nonlinear Schrödinger equation (NLSE) for the pulse envelope [18]:

$$i\partial_z\psi + \gamma|\psi|^2\psi - \beta_2\partial_{tt}\psi/2 = 0 \quad (1)$$

where  $z$  is the propagation distance,  $t$  is the reduced time,  $\beta_2$  is the group-velocity dispersion (GVD) parameter, and  $\gamma$  is the coefficient of cubic nonlinearity of the fibre. This equation neglects the effect of fibre loss, as well as higher-order linear and nonlinear effects. Although these effects can have noticeable impact on pulses shorter than 1 ps, here we neglect them as the leading-order behavior is well approximated by Eq. (1). We consider here a 500 m-long highly nonlinear fibre (HNLF) with the Kerr coefficient  $\gamma = 10 \text{ W}^{-1} \text{ km}^{-1}$  and a low GVD coefficient of  $\beta_2 = 1 \text{ ps}^2 \text{ km}^{-1}$ . With such parameters that are typical of various demonstrations of spectral compression due to SPM in fibre [12], the nonlinearity-dominant regime of propagation is applicable [17]. In this regime, the dispersion term in Eq. (1) plays a relatively minor role and can be neglected. Accordingly, the temporal intensity profile of the pulse does not change along the fibre length, whereas SPM gives rise to a chirp  $\delta\omega_{NL}(t)$  proportional to the temporal gradient of the intensity profile, so that after a propagated distance  $z$ ,  $\delta\omega_{NL}(z,t) = -\gamma P z \partial_t I_{in}$ . The temporal gradients of the various pulse intensity profiles are plotted in Fig. 1 (a2). Note that the nonlinear propagation problem being studied can be conveniently normalized by introducing a normalized distance through the nonlinear length  $1/\gamma P$  associated with the pulse at the entrance of the fibre [17,18]. The resulting temporal chirp of the pulse thus evolves longitudinally as  $\delta\omega(t, z) = A t + \delta\omega_{NL}(z, t) = A t - \gamma P z \partial_t I_{in}$ , which translates in the frequency domain to a modification of the pulse spectrum. The illustration of the impact of the pulse shape on these changes in the spectrum lies at the heart of the present study.

### 2.2. Longitudinal evolution of the pulse spectra

First we examine the evolution of the spectra of the different incident pulses in the HNLF. Fig. 2 summarizes the results and highlights striking differences among the various evolutions. The spectra of the parabolic and Gaussian pulses undergo significant narrowing in the fibre (panels (a) and (b)), and subsequently re-broaden with further propagation. The super-Gaussian and triangular pulses exhibit very different spectral dynamics and do not experience appreciable spectral compression. The extent of the central part of the spectrum of the super-Gaussian pulse does not change much over the fibre length. On the contrary, the spectrum of the triangular pulse shows strong oscillations before splitting into two symmetric parts that move away from each other during propagation.

The very different behaviors of the various waveforms are also reflected in Fig. 3, where we plotted the longitudinal evolution of the spectral brilliance of the pulse at its central frequency (panel (a)) and of the Strehl ratio (panel (b)), defined as the ratio of the spectral peak power of the actual pulse and the spectral peak power obtained assuming a flat temporal phase of the pulse [12,19,20]. It is seen that the parabolic waveform leads to optimum spectral compression, with the spectral brilliance featuring more than thirty-fold increase with respect to the value at the fibre entrance after a propagation distance  $z_P = 334$  m. The Strehl ratio reaches 1 at  $z_P$ , which pinpoints a Fourier transform-limited pulse. The spectral compression performance is degraded for the Gaussian waveform, which achieves a fourteen-fold enhancement in spectral brilliance at the propagation distance  $z_G = 310$  m. The maximum Strehl ratio is 0.24 for this pulse shape, indicating an imperfect compression where the presence of uncompensated temporal chirp of the pulse leads to the appearance of side lobes

Download English Version:

<https://daneshyari.com/en/article/5007310>

Download Persian Version:

<https://daneshyari.com/article/5007310>

[Daneshyari.com](https://daneshyari.com)